Chapter 8

Models of growing cells

Ohad Golan, Hollie J. Hindley, Hidde de Jong, Markus Köbis, Elena Pascual Garcia, and Andrea Weiße

Chapter overview

- A comprehensive description of fundamental growth laws in microbial growth, elucidating the core principles that govern biological growth patterns.
- A detailed exploration of the contrasts between coarse-grained and fine-grained modeling is presented, offering insights into the varying levels of detail that each approach encompasses.
- A thorough breakdown of the key assumptions in the modeling of metabolic systems is provided, underlining the foundational premises that are crucial for accurately representing these complex systems.
- The process of deriving fundamental growth laws by modeling key assumptions is meticulously demonstrated, enabling a clear understanding of how theoretical constructs translate into biological realities.

8.1. Introduction

A key feature of living systems is that they are able to grow and reproduce. The reproductive success in a given environment defines the fitness of a living system. The study of the growth of bacteria and other microorganisms is crucial for better understanding their capacity to cause diseases in humans or for better exploiting their use in biotechnological or environmental processes. Beyond their interest for a variety of applications, bacteria and other microorganisms have shown themselves ideal model systems for investigating fundamental questions on the relation between growth, fitness and characteristics of the environment.

One of the first to systematically and quantitatively study the growth of bacterial cultures was Jacques Monod in the 1940s. He performed so-called diauxic growth experiments, in which bacteria were cultured in a medium containing two different limiting carbon sources. He showed that the bacteria first deplete one carbon source before starting to assimilate the second carbon source. The order in which the primary and secondary carbon source were consumed was determined by the growth rate they support: the preferred carbon source allows the culture to grow at a higher rate. Further work on the molecular basis of diauxic growth led to the discovery that cells inhibit the expression and activity of functions for the use of secondary carbon sources when a preferred carbon source is present, a global regulatory mechanism known as carbon catabolite repression [1, 2].

Monod characterized bacterial growth by means of batch culture experiments in a well-defined growth medium allowing bacteria to reach a state of balanced growth, where the accumulation of biomass can be described

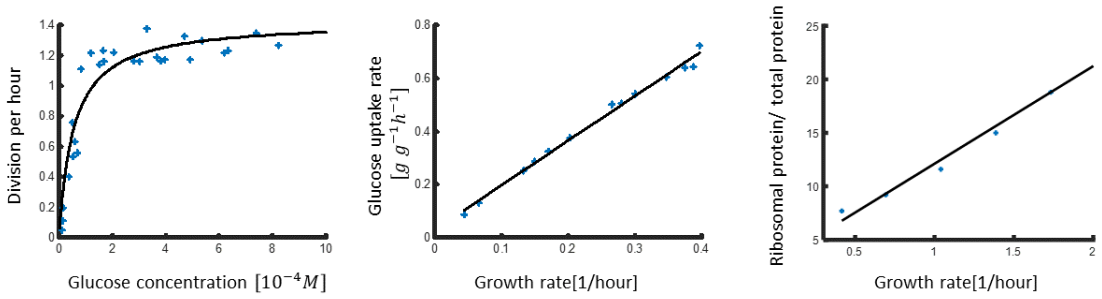

Figure 8.1: Growth laws of bacterial growth. A. Monod growth law: growth rate dependency on nutrient availability [Data from [6]]. B. Correlation between growth rate and nutrient uptake rate [Data from [12]]. C. Correlation between growth rate and cellular composition [Data from [10]]

by a single constant, the exponential growth rate. Together with the chemostat, a device allowing continuous culture of microorganisms at a predefined growth rate [3], these methods have become standard in microbial physiology. They notably underlie the discovery of a number of so-called growth laws, relating the growth rate to a variety of properties of the physiology of growing bacteria. The growth laws are conserved across different organisms and a broad range of experimental conditions. Here, we list three well-known growth laws [4, 5]:

1. *Dependency of the growth rate on nutrient availability* [6]: In his characterization of bacterial growth, Monod discovered the first growth law. He observed that the growth rate of bacteria depends upon the nutrient concentration in the medium in a hyperbolic fashion (Fig. 8.1A).
2. *Correlation between growth rate and nutrient uptake rate* [7]: In continuous cultures, the growth rate was shown to vary linearly with the nutrient uptake rate (Fig. 8.1B). The slope of this linear relation is called the biomass yield and the offset the 'maintenance energy', as it is assumed to be derived from the energy spent on processes required to maintain the basic processes of the cell, in the absence of growth [8].
3. *Correlation between growth rate and cellular composition* [9, 10]: In 1959, Schaechter, Maaløe and Kjeldgaard showed that RNA, DNA and the number of nuclei in *Salmonella typhimurium* linearly correlate with the growth rate. Later, it was further shown that other physiological parameters, such as the mass fraction of ribosomes in growing populations, also linearly correlate with the growth rate [10] (Fig. 8.1C). Initially, it was believed that the correlation between ribosomal mass fraction and growth was strictly positive, however, Scott et al. [11] showed that when growth is inhibited through translation-inhibiting drugs, growth rate and ribosomal mass fraction exhibit a negative (near-)linear relation.

The conserved nature of the growth laws has led scientists to ask whether there are fundamental principles governing bacterial growth. To answer this question, different types of mathematical models have been developed. One approach aims at integrating all known molecular constituents of the cell and the reactions involving these constituents into a big model, an *in-silico* copy, or 'digital twin', of the cell. Such models, known as fine-grained models, can be useful to predict emergent phenotypes, but they are difficult to construct and maintain, and their complexity makes it hard to grasp certain principles that underpin growth. In this chapter, we will focus on coarse-grained models of bacterial growth. Rather than assembling individual reactions in a bottom-up manner, these models are based on the top-down definition of a limited number of basic cellular functions or processes involved in growth, described by appropriate macro-reactions (Fig. 8.2). Coarse-grained models are smaller and therefore easier to construct and analyze. The lack of molecular detail can make their predictions less accurate, but their simplicity allows a focus on how basic cellular functions and their interactions shape bacterial growth. How much detail is included in a model depends

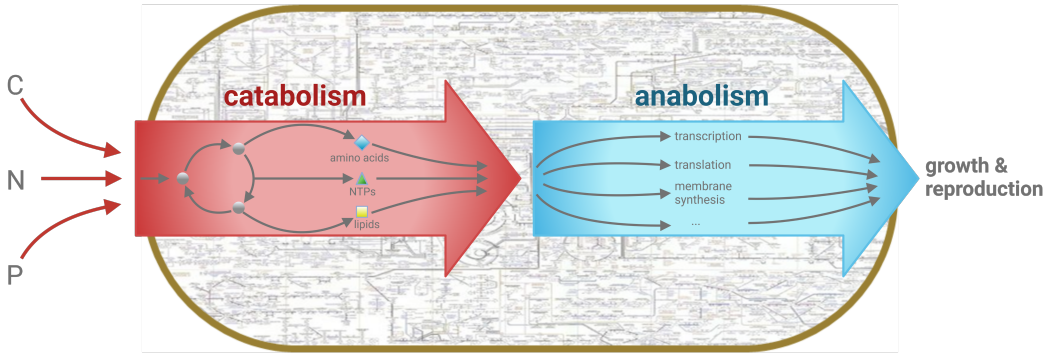

Figure 8.2: Coarse grained modelling of cellular growth. Compared to genome-scale FBA and whole-cell models (Chapters 4, 5, 9, coarse grained models zoom out of the molecular detail and focus on key processes.

on the specific scientific question asked, and similarly, models may vary in their underlying assumptions. Oftentimes, assumptions are based on biochemical principles governing intracellular reactions, on physical limitations faced by cells, on optimality principles, or on a combination of these.

In this chapter, we show how to understand and, ultimately, how to develop coarse-grained models of cellular growth. We present a number of coarse-grained models with increasing levels of granularity. The models have been chosen to also represent a variety of commonly used assumptions, for example, based on growth rate maximization or on phenomenological or mechanistic constraints. Despite these differences, however, models we discuss generally recover the basic growth laws, and we show how the latter can be derived from solving two of the simplest coarse-grained models. The goals of this chapter are:

1. To enable the reader to understand and analyze any model of microbial growth from the literature.
2. To enable the reader to develop their own coarse-grained model of a metabolic system that is directed at their specific scientific question.
3. To provide the reader with a new perspective on modeling of complex systems and specifically the biological cell.

8.2. Fundamental modeling assumptions of microbial growth

The models of microbial growth we consider here are based on fundamental assumptions that follow from biochemical and biophysical constraints. In this section, we discuss and mathematically define assumptions that are found, explicitly or implicitly, in most coarse-grained models of microbial growth. The assumptions are formulated in an abstract manner to hold for any self-replicating biological system, irrespective of the specifics of the underlying molecular mechanisms. In the next section, we use these assumptions to construct increasingly complex models of microbial growth and show how the latter can be used to derive the experimentally observed growth laws presented in the introduction of this chapter.

The growth of microorganisms consists of the uptake of nutrients from the environment and the conversion of these nutrients into new microbial cells through a number of coupled metabolic processes (Fig. 8.2). This description brings out the self-replicating or autocatalytic nature of microbial growth: cells transform nutrients from the environment into new cells. In what follows, we consider growth on the population level, that is, an increase in the total amount of cells or, equivalently in many situations, an increase of the biomass of the population. This leads to the well-known model of microbial growth, where the change in biomass

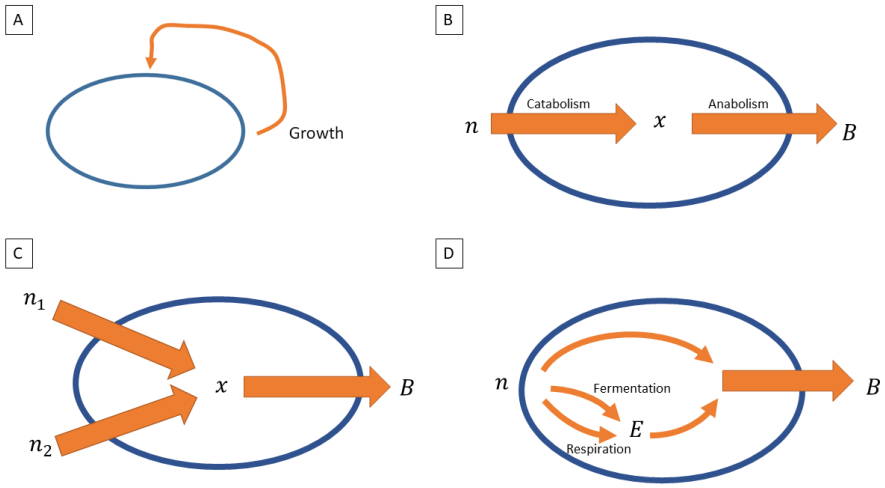

Figure 8.3: Coarse grained models of metabolic systems with increasing complexity. A. A self replicating system. B. The simplest description of a metabolic system: coupled catabolic and anabolic reactions. C. A metabolic system that can catabolize two different nutrient sources. D. A catabolic system requiring two substrates to grow: x and E.

over time is proportional to the amount of biomass (Fig. 8.3A):

$$\frac{\mathrm{d}B}{\mathrm{d}t} = \lambda B, \tag{8.1}$$

where t [h] denotes time, B in gram dry weight [gDW] the biomass and λ [1/h] the population growth rate.

If the growth rate is constant, the solution to Eq. (8.1) describes exponential growth of the biomass:

$$B = B_0 \mathrm{e}^{\lambda t}, \tag{8.2}$$

where B_0 [gDW] is the initial biomass at $t = 0$.

The growth rate is a key parameter that is often used as a proxy for the fitness of microorganisms. It is dependent on the metabolic processes, that is, how a cell utilizes the nutrients to synthesize new biomass (self-replication). The simplest description of metabolism is that it takes up a nutrient, breaks it down into metabolites (catabolism), and then utilizes these metabolites to produce new biomass (anabolism) (Fig. 8.3B). Catabolic and anabolic processes comprise a variety of biochemical reactions that are carried out by different sets of proteins and enzymes. The reaction rates of these processes are limited biochemically and biophysically. We formulate these limitations as modeling assumptions and define them as mathematical constraints, four of which we briefly review below.

8.2.1. Conservation of mass and quasi-steady-state assumption

Dry biomass is often a more readily measurable quantity than cell volume. The latter relates absolute abundances of cell components to their intracellular concentrations. Yet, because bacterial cells have been observed to maintain approximately constant cell density across various growth conditions [13, 14] (though transient exceptions have been observed at the single-cell level [15]), biomass can be regarded a proxy for volume and is therefore assumed to be proportional to cell volume in many growth models. All models considered in this chapter are based on the assumption of constant cell density and approximate the concentration

x of a cellular component x (we use normal font for cell components and italic font for their concentrations) by its absolute abundance divided by the cell mass.

According to the law of mass conservation, the change of mass is equal to the inflow minus the outflow of mass. As a consequence, the change in concentration of a cell component, for example a metabolite pool, is determined by the sum of the rates of the reactions consuming and producing this cell component (Fig. 8.4A). The mass balance for any cell component x is given by the following equation:

$$\frac{\mathrm{d}x}{\mathrm{d}t} = \sum_y r_{y\to x} - \sum_k r_{x\to k}, \tag{8.3}$$

where $r_{y\to x}$ denotes the rate of the reaction converting cell component y into cell component x (production of x), and $r_{x\to k}$ the rate of the reaction converting cell component x into cell component k (consumption of x). Typically, cell component concentrations have units mg/gDW or mmol/gDW, so that rates of metabolic reactions are expressed in units mg/(gDW h) or mmol/(gDW h).

In the simple system shown in Fig. 8.3B, there are two reactions: one converting the nutrient source N into a metabolite X and one utilizing the metabolite for the synthesis of biomass. According to (8.3), the flux balance of metabolite pool x is given by $\mathrm{d}x/\mathrm{d}t = r_{n\to x} - r_{x\to B}$.

A key assumption is that intracellular concentrations are in quasi-steady state. This means that cell component pools remain constant:

$$\frac{\mathrm{d}x}{\mathrm{d}t} = 0, \text{ for all cell components } x. \tag{8.4}$$

The quasi-steady-state assumption simplifies the mathematical analysis of the system significantly and holds for balanced growth of the microbial population. In this chapter, we focus mostly on situations in which the quasi-steady-state assumption applies, but also give an example of a model with metabolic dynamics. In metabolic modeling, the rates of reactions at steady state are called fluxes, denoted by the symbol J. With the quasi-steady-state assumption, Eq. (8.3) becomes

$$\sum_y J_{y\to x} = \sum_k J_{x\to k} \tag{8.5}$$

that is, for every cell component, the sum of production fluxes equals the sum of consumption fluxes. In the example system, we have $J_{n\to x} = J_{x\to B}$.

8.2.2. Proteome allocation assumption

The biochemical reactions breaking down nutrients into intracellular metabolites, and the reactions utilizing these metabolites for the synthesis of new biomass, do not occur spontaneously. The reactions are catalyzed mostly by proteins complexes, in particular metabolic enzymes and ribosomes. In coarse-grained models, well-defined sets of biochemical reactions are grouped together into macro-reactions. The cell components that are necessary to catalyze the individual steps of a macro-reaction are grouped together into a corresponding so-called proteome sector. A proteome sector includes mostly proteins that catalyze metabolic reactions but also ribosomes catalyzing the reaction of protein biosynthesis. Proteins constitute most of the biomass of the cell [16]. Therefore, as a first approximation, the sum of the proteome sectors equals the total biomass of the growing population measured in units of g (Fig. 8.4B):

$$\sum_{r\in\{x\to y\}} P_r = B, \tag{8.6}$$

where $P_{x\to y}$ is the proteome sector catalyzing the macro-reaction that transforms cell component x into cell component y. The proteome sectors as defined above are extensive quantities, summed over the entire growing population, like the total biomass B. For the models, we are rather interested in intensive quantities, the amount of a proteome sector relative to the total amount of biomass (protein), corresponding to protein concentrations or protein fractions. Dividing the left-hand and right-hand sides of Eq. (8.6) by B, we thus obtain:

$$\sum_{r\in\{x\to y\}} p_r = 1 \tag{8.7}$$

where $p_{x\to y}$ is the fraction of the proteome converting x into y, defined by $p_{x\to y} = P_{x\to y}/B$. Proteome fractions are dimensionless and sum to one.

In the simple example system in Fig. 8.3B, we distinguish two macro-reactions: a catabolic reaction and an anabolic reaction (biomass synthesis). We therefore define two proteome sectors, corresponding to enzymes and ribosomes, respectively, with fractions $p_{n\to x}$ and $p_{x\to B}$, respectively. In later examples in the chapter, the catabolic and anabolic processes are further broken down into smaller macro-reactions and so are the proteome sectors.

8.2.3. Mathematical description of reaction fluxes

The rate at which a reaction is converting one cell component, e.g., a metabolite, into another is determined by the proteome fraction, the concentrations of the substrates of the reaction and possible regulation by other cell components in the system. While mass-action kinetics provide a principled framework to develop rate equations for biochemical reactions, in practice, various approximations based on mechanistic assumptions are often used to obtain simplified equations [17]. Below there are a few examples of rate laws defining the fluxes in coarse-grained models:

1. *Excess substrate and no allosteric interactions.* The simplest relation of the flux J to the relevant proteome sector is linear, such that

$$J_{x\to y} = p_{x\to y}\,\beta_{x\to y}, \tag{8.8}$$

   where $\beta_{x\to y}$ is a parameter describing the efficiency of proteome sector $p_{x\to y}$ in generating a flux from x to y. This expression assumes substrate x is in excess and disregards any regulation of the flux by allosteric interactions of the enzymes and other cell components.
2. *Limited substrate and allosteric interactions.* A more complex relation is obtained when the substrate is in excess and allosteric interactions involving a cell component n play a role in the modulation of the flux. The expression of the flux is multiplied by two regulatory functions $f(x)$ and $g(n)$ describing the modulation of the flux by the substrate and the allosteric cell component, respectively:

$$J_{x\to y} = p_{x\to y}\,\beta_{x\to y}\,f(x)\,g(n). \tag{8.9}$$

   It is important to note that that both $f(x)$ and $g(n)$ return values between 0 and 1, and that the flux remains linear in the proteome fraction. Typically, a Michaelis-Menten relation is taken for the effect of the concentration of substrate x on the flux, such that $f(x) = x/(k_{x\to y} + x)$ (Fig. 8.4D). When the concentration x is in excess, such that $x \gg k_{x\to y}$, the function $f(x)$ becomes approximately 1. Other types of regulatory functions can be used depending on the macroreactions concerned and the growth conditions.

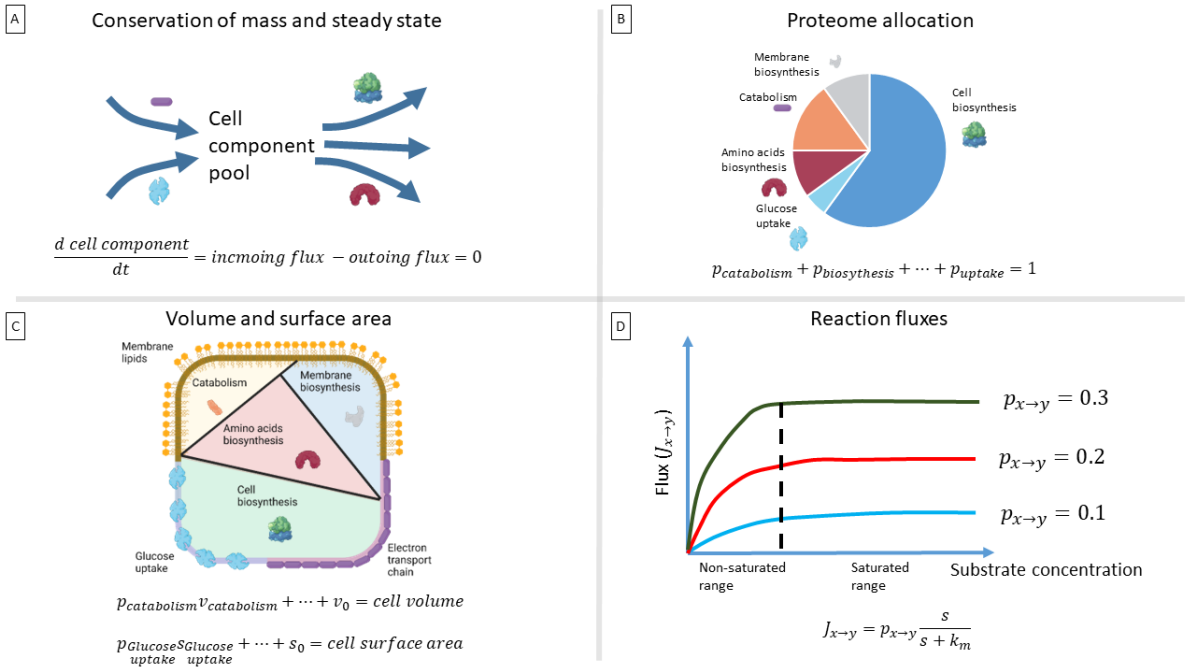

Figure 8.4: Fundamental assumptions in the modeling of microbial growth. A. Conservation of mass and steady-state assumption: The change in concentration of a cell component is equal to the incoming flux minus the outgoing flux. At steady state, the concentration of the cell component is constant. B. Proteome allocation assumption: the proteome is divided into different proteome sectors. The number of proteome sectors in a model depends on the model granularity. The sum of all the proteome sectors always equals 1. C. Volume and surface area assumption: The volume of the cell is limited and is filled with intracellular cell components such as proteins. The sum of the volumes of the intracellular cell components is equal to the cell volume. Similarly, the surface area of the cell is limited and contains membrane cell components such as lipids. The sum of the surface areas of membrane cell components is equal to the cell surface area. D. Example of flux assumption according to Michaelis-Menten kinetics: the reaction $x \to y$ is carried out by proteome sector $p_{x\to y}$. The maximal rate is reached for saturating substrate concentrations and is determined by the size of the proteome sector.

8.2.4. Volume and surface area assumptions

The intracellular volume as well as the surface area of the cell are limited (Fig. 8.4C). Obviously, the total volume occupied by the components of the cell, in particular proteins, cannot be larger than the cell volume. As such, the total volume of the cell is larger than the sum of the volume of the proteome sectors that are functioning inside the cell plus some constant volume taken up by other cell components such as DNA. This gives the following constraint:

$$\text{Cell volume} \geq \sum_{r\in\{x\to y\}} p_r v_r + v_0 \tag{8.10}$$

where $v_{x\to y}$ is the volume of proteome sector $p_{x\to y}$ and v_0 is some constant volume filled by other cell components. Similarly, the total surface occupied by proteins and lipids making up the cell membrane has to equal the surface area of the cell. This constraint gives:

$$\text{Cell surface area} \geq \sum_{r\in\{x\to y\}} p_r s_r + l_0 \tag{8.11}$$

where $s_{x\to y}$ is the surface area of proteome sector $p_{x\to y}$ and l_0 is the surface area of the lipids in the cell membrane.

8.3. Derivation of growth laws from basic modeling assumptions

In the following section, we will build upon the fundamental assumptions discussed earlier to construct models of microbial metabolism with increasing complexity. We will introduce additional assumptions as necessary to solve each model, and use them to derive one of the growth laws presented in the introduction of this chapter that have been experimentally observed in microorganisms.

Example 1 - Basic metabolic system with saturating substrate concentrations
In this example, we will use the basic metabolic model to derive the relationship between the concentration of ribosomes and the growth rate in microorganisms.The most basic metabolic model involves the uptake of a single nutrient from the environment, the catabolism of that nutrient into a metabolite x, and the use of this metabolite in anabolic processes to synthesize biomass (Fig. 8.3B). This model consists of two reactions and two proteome sectors. According to the proteome allocation constraint, the sum of the proteome sectors must sum to one (according to Eq. (8.7)):

$$p_{n\to x} + p_{x\to B} = 1. \tag{8.12}$$

For simplicity, we assume that the rate of each reaction is proportional to the allocation of the proteome to that reaction (according to Eq. (8.8)), so that:

$$J_{n\to x} = p_{n\to x}\beta_{n\to x}; \quad J_{x\to B} = p_{x\to B}\beta_{x\to B}. \tag{8.13}$$

The mass conservation constraint, with the assumption of a steady state for metabolite x, gives (according to Eq. (8.5)):

$$J_{n\to x} = J_{x\to B}. \tag{8.14}$$

Finally, due to conservation of mass, the biomass synthesis flux equals the growth rate:

$$\lambda = J_{x\to B}. \tag{8.15}$$

Solving equations (8.12)-(8.15) gives a prediction for the growth rate:

$$\lambda = \frac{\beta_{x\to B}\beta_{n\to x}}{\beta_{x\to B} + \beta_{n\to x}}. \tag{8.16}$$

Solution (8.15) for the growth rate is based solely on *mechanistic assumption* - that is, assumptions that are based on the mechanistic properties of the biochemical reactions in the cell. In this case, that is that the fluxes are linear to the relevant proteome sector. Because we have taken a steady state approximation and the rates of the two reactions must be equal, the growth rate is determined by the relative values of the catalytic constants.

Using this model, we can now derive the relationship between the concentration of ribosomes and the growth rate. Combining Eq. (8.12) and (8.14) gives:

$$\lambda = p_{x\to B}\beta_{x\to B} \tag{8.17}$$

This shows that the growth rate is linearly proportional to the anabolic sector. Given that the anabolic sector

is composed mostly of ribosomes, this fits well with the experimentally observed linear relationship between the concentration of ribosomes and the growth rate, which was first described by Schaechter *et al.* [9] and later confirmed by Bremer *et al.* [10]. It is important to notice that this relation is due to the assumption that the biomass synthesis flux is linear in the ribosomal proteome sector.

In summary, we have derived the linear relationship between the concentration of ribosomes and the growth rate using only basic assumptions about the properties of the biochemical reactions in the cell and the conservation of mass. This relationship is one of the experimentally observed growth laws in microbial systems.

Example 2 - Growth on two nutrient sources

In this example, we consider a metabolic system that grows on two different nutrient sources, n_1 and n_2 Fig. 8.3C. We use the fundamental assumptions outlined in Section 1.2 and an additional assumption of growth-rate maximization to demonstrate how cells may exhibit catabolite repression - a phenomenon in which cells utilize only one nutrient even when multiple nutrients are available in the environment [2].

The metabolic system in this example catabolizes both nutrient sources to the same metabolite x, but at different efficiencies. The anabolic reaction is the same as in Example 1. There are now three proteome sectors in this model: two for catabolism of the nutrients and one for anabolism. Thus, according to the proteome allocation constraint (Eq. 8.7), we have:

$$p_{n_1\to x} + p_{n_2\to x} + p_{x\to B} = 1. \tag{8.18}$$

As before, we assume a linear correlation between reaction rates and proteome sector fractions (according to Eq. (8.8)). The different efficiencies of the catabolic sectors is represented as $\beta_{n_2} > \beta n_1$. Applying the mass conservation assumption for metabolite x, combined with the steady state assumption, gives

$$J_{n_1\to x} + J_{n_2\to x} = J_{x\to B}. \tag{8.19}$$

The growth rate is again equal to biomass synthesis flux, as in Example 1:

$$\lambda = J_{x\to B}. \tag{8.20}$$

Given that there are more variables than constraints in this example, solving Eqs. 8.18 - 8.20 reveals that there is no unique solution for the growth rate, but rather a solution space with one free variable $p_{n_1\to x}$:

$$\lambda = \frac{\beta_{x\to B}\beta_{n_2\to x}}{\beta_{x\to B}+\beta_{n_2\to x}} + p_{n_1\to x}\left(\frac{\beta_{n_1\to x}-\beta_{n_2\to x}}{\beta_{x\to B}+\beta_{n_2\to x}}\right)\beta_{x\to B}. \tag{8.21}$$

The solution shows that the metabolic system has a decision to make regarding how much of the proteome to invest in sector $p_{n_1\to x}$. To solve this system, we introduce an additional assumption of *growth rate maximization* – that is, to maximize its fitness, the metabolic system maximizes the growth rate in a given condition. In this example, to maximize the growth rate, the cell uses only the more efficient catabolic system, setting $p_{n_1\to x} = 0$ and the solution for the growth rate is as in example 1. The model predicts that the cells will only utilize the nutrient source with the higher efficiency, even if both nutrient sources are available in the environment. This solution fits the catabolic repression experimental result presented in the introduction in which in which the metabolic system represses the use of a less efficient nutrient source in favor of a more efficient one.

Example 3 - Multiple energy generating pathways

In this example, we focus on a classic question in cell physiology known as overflow metabolism [18, 19]. Within the cell, two primary energy-generating pathways exist: the oxygen-requiring respiration pathway and the oxygen-independent fermentation pathway. It is established that, in the presence of oxygen, the respiration pathway fully oxidizes available nutrients, rendering it more nutrient-efficient in contrast to the fermentation pathway [20]. Utilization of the fermentation pathway is marked by the secretion of byproducts, such as acetate in *E. coli* or ethanol in yeast, making it inherently wasteful. Intriguingly, experimental observations reveal a counterintuitive phenomenon: even under oxygen-rich conditions, cells often opt for the less efficient fermentation pathway. Under growth rates surpassing a critical threshold, the secretion rate of byproducts, indicating an increased reliance on the fermentation pathway, exhibits a linear rise [21, 22, 23]. This counterintuitive preference for fermentation has long presented a profound question in bacterial physiology.

Based on previous studies [21], we present a coarse-grained model to elucidate this observed phenomenon (Fig. 8.3D). The model postulates steady-state growth on a single nutrient source, denoted as n. This nutrient is taken up from the environment, and channeled towards biomass through the proteome sector $p_{n\to B}$. Additionally, it serves as a precursor for energy generation, either through the respiration pathway catalyzed by proteome sector $p_{n\to r}$ or the fermentation pathway catalyzed by proteome sector $p_{n\to f}$. Thus, according to the proteome allocation constraint (Eq. 8.7), we have:

$$p_{n\to B} + p_{n\to r} + p_{n\to f} = 1. \tag{8.22}$$

Diverging from earlier models presented in this chapter, our model necessitates two precursors for biomass generation: energy and a carbon precursor. Carbon assimilation is coarse-grained into the biomass generation pathway $n \to B$, while energy is generated through the energy-producing pathways of respiration $n \to r$ and fermentation $n \to f$. Consequently, two mass balance equations are requisite – one for carbon flux and another one for energy flux. The carbon mass balance equates the carbon uptake rate coming from nutrient uptake J^C_{in} to the carbon fluxes utilized for cell biosynthesis $J^C_{n\to B}$, fermentation $J^C_{n\to f}$ and respiration $J^C_{n\to r}$:

$$J^C_{in} = J^C_{n\to B} + J^C_{n\to f} + J^C_{n\to r}. \tag{8.23}$$

Similarly, the energy balance equation asserts that the energy generated by fermentation $J^E_{n\to f}$ and respiration $J^E_{n\to r}$ equals the energy utilized for the biomass synthesis reaction $J^E_{n\to B}$:

$$J^E_{n\to B} = J^E_{n\to f} + J^E_{n\to r}. \tag{8.24}$$

Consistent with prior examples in this chapter, we maintain a linear correlation between reaction rates and proteome sector fractions (as per Eq. 8.8).

Both fermentation and respiration reactions utilize a carbon substrate and produce energy, with a key distinction lying in their nutrient utilization efficiency. The ratio of carbon utilized in these reactions to energy generated is expressed as:

$$J^E_{n\to r} = \epsilon_{n\to r} J^C_{n\to r}; \quad J^E_{n\to f} = \epsilon_{n\to f} J^C_{n\to f}. \tag{8.25}$$

Given that the respiration pathway exhibits higher nutrient efficiency than the fermentation pathway: $\epsilon_{n\to r} > \epsilon_{n\to f}$.

Concluding the model description, we incorporate the cellular requirements for growth precursors (energy and carbon) and the proteome. Under carbon limitation, the proteome fraction dedicated to cell biosynthesis $p_{n\to B}$ exhibits a linear growth rate dependence [21, 24, 11, 25]:

$$p_{n\to B} = p_0 + \sigma_{n\to B}\lambda. \tag{8.26}$$

The growth rate correlates with the flux of growth precursors, adhering to a fixed stoichiometry of the metabolic network [26, 27]:

$$J^E_{n\to B} = \sigma_E\lambda; \quad J^C_{n\to B} = \sigma_C\lambda. \tag{8.27}$$

Another key assumption of the model posits that, while the respiration pathway is more nutrient-efficient, utilizing less nutrients per energy unit generated, the fermentation pathway is more proteome-efficient, requiring a smaller proteome fraction per energy unit generated. This assumption is embodied in the efficiency parameters of the reaction fluxes: $\beta_{n\to f} > \beta_{n\to r}$.

To validate the efficacy of our model in capturing the experimentally observed linear increase in acetate secretion with high growth rates, we endeavored to predict acetate secretion as a function of growth rate. The acetate secretion rate is governed by the flux through the fermentation pathway, represented by $J_{ac} = S_{ac}J^C_{n\to f}$, where S_{ac} is determined by the involved stoichiometry. Solving Eqs 8.22 - 8.27 for acetate secretion yields an expression that increases linearly with the growth rate:

$$J_{ac} = \frac{S_{ac}}{\epsilon_{n\to f}}\beta_E(p_E - \lambda(\sigma_{x\to B} + \frac{\sigma_E}{\beta_{x\to r}})). \tag{8.28}$$

where $\beta_E = \frac{\beta_{n\to r}\beta_{n\to f}}{\beta_{n\to r}-\beta_{n\to f}}$ and $p_E = 1 - p_0$. The negative value of β_E, arising from the higher proteome efficiency of the fermentation pathway, results in a positive slope and a negative intercept on the J_{ac}-axis. The model provides a good quantitative fit to the experimental observation [21]. The critical growth rate λ_{cr}, signifying the growth rate at which the cell activates the fermentation pathway, occurs when $J_{ac} = 0$, giving $\lambda_{ac} = \frac{p_E}{\sigma_{n\to B}+\sigma_E/\beta_{n\to r}}$.

It is crucial to highlight the key assumption underlying this solution, which lies in the relative efficiencies of the energy-generating pathways. At high growth rates, the cell encounters inhibition not only in its ability to rapidly extract energy from the nutrient but, more significantly, it is constrained by the available proteome. Consequently, the cell shifts to utilize the more efficient fermentation pathway.

It is also noteworthy to identify the assumptions overlooked by the model. For instance, the model excludes the proteome sector for nutrient uptake, coarsely integrating it into the biomass biosynthesis and energy generation pathways. While this assumption is reasonable for growth on a single nutrient, a model considering multiple nutrients with varying uptake efficiencies necessitates the inclusion of proteome sectors for nutrient uptake. Further analysis of the model can be found in [21, 28].

8.4. Mechanistic links between cellular trade-offs, gene expression, and growth

This section presents a coarse-grained cell model that describes the dynamic adaptation of global mechanisms driving the growth of bacterial cells. Compared to the models previously described in this chapter, this model is dynamic, i.e. not based on steady-state assumptions, and it has a higher level of granularity. It is also based on explicit mechanisms, which allows extension with additional mechanisms of interest, for example,

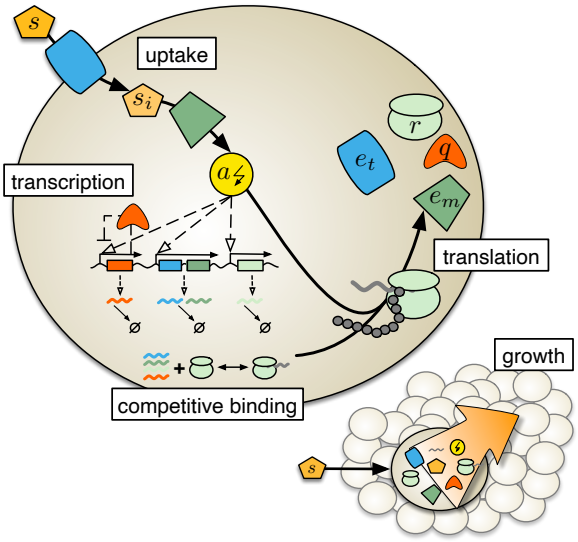

Figure 8.5: Schematic of the dynamic growth model. The model focuses on key cellular processes: nutrient uptake, transcription and translation. Enzymes (shown in blue and dark green) import and metabolize extracellular nutrient (shown in orange), which yields energy (yellow). Availability of energy impacts transcription and translation, however, it is assumed that energy consumption is dominated by translation. The different species of mRNA compete for ribosomes (light green), and their translation consumes energy. Assuming that biomass is dominated by protein, the total rate of translation determines the rate of growth (lower right). Four classes of proteins are modelled: ribosomes, nutrient transporters, enzymes and other house-keeping proteins (red).

the effects of antibiotics or of heterologous gene expression on cellular growth.

Energy metabolism and protein production are the main pillars of biomass production and cell growth, and form the basis of the growth model. A set of ordinary differential equations describes the dynamic interplay of (i) nutrient internalization and catabolism, (ii) transcription, and (iii) and translation (see Fig. 8.5). A key assumption of the model is that biomass is dominated by proteins, and so the cellular growth rate corresponds to the total rate of protein synthesis via translation. All processes are part of a feedback loop in which the final protein products act as catalyzers of the model reactions, creating a self-replicating system.

In its basic form, the growth model includes 14 intracellular variables: internal nutrient, s_i; energy molecules, a; and four types of proteins along with their corresponding free (m_x) and ribosome-bound mRNAs (c_x). Of the four types of proteins considered, there are three groups of catalyzing molecules: transporters (e_t), metabolic enzymes (e_m) and ribosomes (r), and one group of housekeeping proteins (q). As the model does not assume steady state, the different reactions are defined in terms of reaction rates instead of reaction fluxes. A simplified description of the main reaction rates of the model is shown in Table **??**. For details on all reactions and parameters, readers are referred to the supplementary information of [29]. In what follows, the focus will be on the conceptual aspects underlying the prediction of cellular growth rate, and some examples of model applications.

Building on the assumptions of mass balance and proteome allocation described in Section 8.2 of this chapter, the model centers around three fundamental constraints, namely (i) a finite pool of cellular energy that fuels protein biosynthesis, (ii) a finite pool of ribosomes for which mRNAs compete for translation, and (iii) a finite cell mass. As a result, the model predicts the dynamic allocation of internal resources and its emergent impact on cellular growth rate without the need to assume growth rate maximisation.

Description	Reaction	Reaction rate
Nutrient internalisation	$s \rightarrow s_i$	$e_t \cdot \frac{v_t s}{(K_t+s)}$
Nutrient metabolism	$s_i \rightarrow n_s a$	$e_m \cdot \frac{v_m s_i}{(K_m+s_i)}$
Transcription	$\varnothing \rightarrow m_x$	$\omega_x \cdot \frac{a}{(\theta_x+a)}$
Ribosome binding	$m_x + r \leftrightarrow c_x$	$k_b \cdot m_x r,\ k_u \cdot c_x$
Translation	$c_x + n_x a \rightarrow x + m_x + r$	$c_x \cdot \frac{\gamma(a)}{n_x}$

Table 8.1: Summary of main model reactions and their accompanying rates. The four proteins represented in the model are denoted in the reactions by x, $x \in r, e_t, e_m, q$, $\gamma(a)$ is the rate of translational elongation, defined as $\frac{\gamma_{max} a}{K_\gamma + a}$, and n_x is the average length of a protein molecule in amino acids. The parameter n_s represents nutrient quality and determines the yield of energy per catabolized nutrient.

8.4.1. Model definitions

Growth rate and biomass synthesis Based on the assumption that biomass is dominated by protein, and other contributions are negligible, the biomass B of a cell can be calculated by summing over the coarse-grained proteome,

$$B = \sum_x n_x x + n_r \sum_x c_x, \qquad x \in r, e_t, e_m, q, \tag{8.29}$$

which sums over all proteins (x) and mRNA-bound ribosomes (c_x), with n_r and n_x denoting the lengths of proteins in terms of amino acids. Equation (8.29) is equivalent to the mass balance assumption described in section 1.2.1 of this chapter. As a consequence, the proteome allocations, defined by $\phi_x = x/B$ for $x \in \{e_m, e_t, r, q\}$ sum to 1, i.e. $\sum_x \phi_x = 1$.

Similar to the previous examples in this chapter (Section 8.3), the model correlates the growth rate with biomass production, which depends on translating ribosomes and their translation elongation rate $\gamma(a)$. Importantly, the rate of elongation depends on the energy produced in the catabolic processes described in the model, which dynamically couples protein synthesis with metabolism. Defining the number of translating ribosomes $R_t = \sum_x c_x$, the change in cellular biomass over time becomes

$$\frac{dB}{dt} = \gamma(a) R_t - \lambda B. \tag{8.30}$$

The second term, λB, accounts for dilution via redistribution of mass to daughter cells at division. In homeostatic conditions, that is when B is in steady state and so $\frac{dB}{dt} = 0$, it then follows that λ^* is proportional to the rate of protein synthesis. To define growth dynamically,

$$\lambda(t) := \frac{\gamma(a) R_t}{B_0}, \quad B_0 > 0. \tag{8.31}$$

Setting B_0 to the typical biomass of a cell in mid-exponential growth ensures that cells will have a steady-state biomass of $B^* = B_0$.

Rate of translation In actively growing bacteria, protein synthesis, and in particular translation-associated processes, account for a major part of the energy budget. The model assumes a simplified mechanism to derive the dependence of the translation rates on the energy levels of the cell. It is assumed that each elongation step of translation consumes a fixed amount of energy (Figure 8.6),

and further that intermediate reactions are in quasi-steady state. It can then be shown that the net rate of

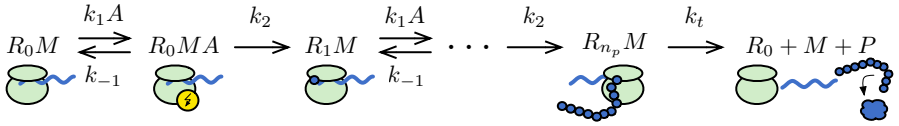

Figure 8.6: Mechanistic derivation of the translational elongation rate. The model assumes that each elongation step consumes a fixed amount of energy. In a first step, energy reversibly binds the mRNA-ribosome complex, upon which elongation takes place. Once the peptide reaches it's final length, the protein is released and ribosome and mRNA are freed up.

translation elongation takes the form

$$\gamma(a) = \frac{\gamma_{\max} a}{K_\gamma + a}. \tag{8.32}$$

Here, $\gamma_{\max}$ denotes the maximal rate of translation elongation per ribosome and K_γ the energy threshold of half-maximal elongation. For any protein x, the rate of its translation is then given by

$$\nu_x(c_x, a) = c_x \frac{\gamma(a)}{n_x}, \tag{8.33}$$

where c_x denotes ribosomes bound to mRNA of type x and division by n_x accounts for the number of elongation steps to take place for the production of one p_x.

Rate of transcription The model assumes that transcription is energy-dependent, but that its consumption is negligible compared to that of translation. Analogous to translation, under the assumption of fixed energy consumption per elongation step, the rate of transcription takes the same shape and is defined by

$$\omega_x(a) = \frac{\omega_x a}{\theta_x + a}, \qquad x \in r, e_t, e_m. \tag{8.34}$$

Here, the energy threshold of half-maximal transcription, θ_x, is specific for each proteome sector x, which dynamically links the proteome allocations ϕ_x with different growth conditions. In particular, $\theta_r \gg \theta_x$ for $x \neq r$ ensures that the ribosomal sector increases in rich growth conditions (cf. growth laws in Fig. 8.1C).

In addition, the model assumes that the transcription of household genes is negatively auto-regulated to maintain near constant levels across different conditions. Therefore

$$\omega_q(q, a) = \frac{w_q a}{\theta_q + a} \cdot \mathcal{I}(q), \qquad with \quad \mathcal{I}(q) := \frac{1}{1 + (q/K_q)^{h_q}}, \tag{8.35}$$

where $\mathcal{I}$ is the auto-inhibition function with threshold K_q and Hill-coefficient h_q.

8.4.2. Model predictions

The model recovers the bacterial growth laws through the automodulation of finite cellular resources in response to changing environments. It robustly fits empirical data (Fig. 8.7), suggesting the growth laws are an emerging property of the constraints integrated into the modelling approach.

The model predicts a hyperbolic dependence of the growth rate on nutrient availability as described by Monod's law (Fig. 8.7 inset), derived using the conservation of mass assumption and when $\phi_r \ll \phi_q$. Energy is created from the metabolism of internalized nutrients and determines the rates of transcription ($\omega_x(a)$) and translation ($\gamma(a)$). In the absence of antibiotics, the latter is proportional to the growth rate of the cell as described in Eq. (8.31). As the nutrient quality is increased, more energy will be available and therefore more

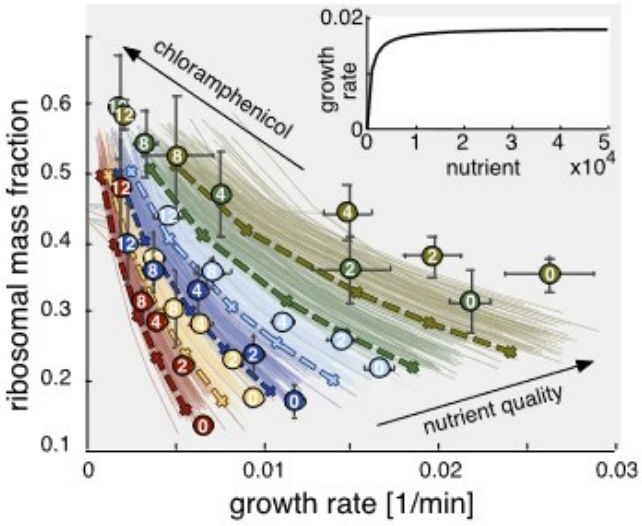

Figure 8.7: Experimental data [coloured circles] and model simulations [lines] depicting the relationship between growth rate and cellular composition. The data describes the ribosomal fraction of the proteome ϕ_r in different growth conditions. Each colour represents a different media composition, with increasing drug-free growth going from red to green. The numbers within the circles indicate the addition of the antibiotic chloramphenicol to the growth media at a certain concentration [in μM]. Although this antibiotic inhibits translation, an increase in ϕ_r can be observed through all media compositions. The model fit to the experimental data demonstrates the capacity of this model to describe two of the growth laws. (Inset) Model simulation. Besides the composition, varying the amount of external nutrient in the growth media increases the steady-state growth rate up to a saturation point. This reproduces Monods growth law.

transcription will occur. Due to the relationship between transcription thresholds ($\theta_r \gg \theta_x$), the transcription of ribosomes is increased comparatively more, leading to an increase in the ribosomal mass fraction as seen in Fig. 8.7.

In a fixed nutrient condition, inhibiting translation by the addition of an antibiotic increases intracellular energy levels as fewer ribosomes can translate. Again, with $\theta_r \gg \theta_x$, this energy increase leads to a proportionally larger increase in transcription of ribosomal mRNAs and so to a larger ϕ_R. In contrast to the scenario without antibiotics, fewer ribosomes can actively translate and therefore the growth rate will be lower. Consequently, a negative dependence of ϕ_R and growth rate arises.

8.4.3. Applications

Due the coarse-grained modelling of mechanisms and the use of non-steady state dynamics, the model lends itself to modular extension for a range of applications. For example, to reproduce the negative correlation between growth rate and ribosome content amid translational inhibition (Fig. **??**), the model was extended to account for inhibitory actions of the antibiotic chloramphenicol on ribosomes. Similarly, mechanisms that account for drugs with other modes of action could also be included. Further, in [29], it was shown that the model can be extended to study a number of applications:

Firstly, the model was extended to account for expression of a heterologous gene circuit and predict constraints between heterologous circuit expression, circuit function, and the growth of the host. This has applications in areas such as chemical production in biotechnology, where host-circuit interactions are not understood and where synthetic circuits have to operate robustly in different growth conditions. In this context, the model can serve to quantify host-circuit interactions for a more host-aware design of synthetic gene circuits.

In another application, the model's ability to dynamically predict growth rate emergently from intracellular mechanisms was used as a proxy for evolutionary 'fitness' to study when gene regulation was evolutionarily stable. This was done by augmenting the cell model with population growth, assuming that all cells of a population are identical, and modelling competitive interactions between a resident and mutant strain.

Finally, in [29] it was shown how to use the model to study specific mechanisms within a wider cellular context. With the example of gene-dosage compensation, where the effects of a gene deletion can be reduced by increasing the expression of a paralogous gene, it was shown how and when global regulatory mechanisms caused compensation. The example showed that the constraints underpinning the growth laws can also cause global negative feedbacks on proteins affecting growth.

8.5. Concluding remarks

In this chapter, we delved into the intricate world of coarse-grained modeling of microbial growth. We began by describing key experimental evidence that has led to what is known as bacterial growth laws. These laws are derived from growth measurements and are deemed to be conserved for various organisms. We then mathematically described the fundamental assumptions necessary to model bacterial growth. Using basic modeling systems, we showed how to analyze such a system and derive fundamental conclusions for bacterial growth. These models reproduce the bacterial growth laws, providing a link between theoretical models and experimental results. Finally, we introduced a more complex model that includes various cell processes such as translation, transcription, and the cellular growth process. Overall, this chapter highlights the power of coarse-grained modeling in unraveling the complexities of microbial growth and offers a framework for exploring a wide range of biological questions.

While this chapter lays a foundation for research on various topics in biology, many areas remain to be explored. For example, the effects of changing environmental conditions such as dynamic changes in nutrient availability, acidity, or temperature are not discussed. Furthermore, various cellular processes such as protein degradation and membrane assembly are not covered in the chapter. Including these processes in a coarse-grained model could potentially lead to the discovery of other growth laws.

In the next chapter, you will explore models that further refine the biological cell and bridge between coarse-grained models and genome-scale models. These models incorporate several of the assumptions discussed here but utilize more knowledge of the metabolic network.

Recommended readings

Growth laws in microbiology:

- Monod, The growth of bacterial cultures, *Annual Review of Microbiology*, 1949 [6]. Classical reference for the quantitative modeling of microbial growth.
- Schaechter, Maaløe, and Kjeldgaard, Dependency on medium and temperature of cell size and chemical composition during balanced growth of *Salmonella typhimurium*, *Microbiology*, 1958 [9]. Classical article that introduced the growth law for ribosomes.
- Scott, Gunderson, Mateescu, Zhang, and Hwa. Interdependence of cell growth and gene expression: origins and consequences, *Science*, 2010 [11]. Article that renewed interest in growth laws for the quantitative study of microbial physiology.
- Jun, Si, Pugatch, and Scott, Fundamental principles in bacterial physiology – history, recent progress, and the future with focus on cell size control: a review, *Reports on Progress in Physics*, 2018 [4]. Recent and very complete review of growth laws in microbiology.

Coarse-grained modeling of microbial growth:

- Hinshelwood, On the chemical kinetics of autosynthetic systems, *Journal of the Chemical Society*, 1952 [30]. Historical reference for coarse-grained modeling of microbial growth.
- Kafri, Metzl-Raz, Jonas and Barkai, Rethinking cell growth models, *FEMS Yeast Research*, 2016 [31]. Recent review of coarse-grained models of microbial growth.
- de Jong *et al.*, Mathematical modelling of microbes: metabolism, gene expression and growth, *J. R. Soc. Interface*, 2017 [32]. Recent review comparing coarse-grained models of microbial growth with other modeling frameworks.
- Bruggeman, Planqué, Molenaar, and Teusink, Searching for principles of microbial physiology, *FEMS Microbiology Reviews*, 2020 [33]. Recent review summarizing biological insights obtained from coarse-grained models.

Examples of coarse-grained models:

- Molenaar, van Berlo, de Ridder and Teusink, Shifts in growth strategies reflect tradeoffs in cellular economics, *Molecular Systems Biology*, 2009 [34]. Influential article illustrating the explanatory capacity of coarse-grained models.
- Weiße *et al.*, Mechanistic links between cellular trade-offs, gene expression, and growth, *Proceedings of the National Academy of Sciences of the USA*, 2015 [29]. Article describing how growth laws for ribosomes can be recovered from coarse-grained model of microbial growth.
- Basan *et al.*, Overflow metabolism in *Escherichia coli* results from efficient proteome allocation, *Nature*, 2015 [21]. Article describing how proteome allocation constraints can account for overflow metabolism in bacteria.
- Zavřel *et al.*, Quantitative insights into the cyanobacterial cell economy, *eLife*, 2019 [35]. Example of the use of coarse-grained models for explaining physiological principles underlying growth of less-studied (photosynthetic) microorganisms.

Problems

Problem 8.1 A linear chain model A system is composed of a set of 2 linear reactions: nutrient -> metabolite x_1 -> metabolite x_2 -> biomass. Using the same approximations as in example 1, solve for the growth rate. What would be the solution for a system composed of N reactions? Show that the least efficient reaction determines the growth rate.

Problem 8.2 A linear chain model with Michaelis-Menten rate laws Solve example 1 when the nutrients are not available in excess. Use Michaelis-Menten relations for both reactions. First, derive the concentration of metabolite x as function of catabolic sector proteome size. What is the minimal size for the catabolic sector? What happens if the catabolic sector is smaller than that? Next, determine the proteome allocation that maximizes the growth rate.

Problem 8.3 A linear chain model with Michaelis-Menten rate law for the catabolic reaction Solve Example 2 when the nutrients are not available in excess. Use Michaelis-Menten relations for the catabolic reaction. At what point does the metabolic system switch to use the other nutrient source?

Problem 8.4 A simple model with allosteric regulation of catabolic reaction([36]): A metabolic system is growing in an environment with one nutrient available. The system allosterically regulates its catabolic reaction according to the concentration of metabolite x. Assume Michaelis-Menten kinetics for all reactions. What is the growth rate as function of catabolic sector proteome size? This is a complex solution, don't solve it analytically and plot a numerical solutions instead. What is the catabolic sector proteome size that

maximizes the growth rate?

Problem 8.5 Growth on a single nutrient that is degraded to both energy and biomass precursors Consider the model from section 1.3, example 3. Solve the model for the nutrient uptake rate as function of growth rate for:

1. Growth rates above the onset of acetate secretion.
2. Growth rates below the onset of acetate secretion.

Problem 8.6 Simulating models numerically Simple coarse-grained models can generally be solved analytically. However, for models with a higher level of granularity, like the one presented in this section, reaching an analytical solution to the model equations is highly complex. Computational approaches that allow numerically solving high-dimensional systems are of great value.

1. With the help of the provided code and following the detailed description of the ODE system in the SI of [29], implement and solve the system of ODEs. Using this implementation, reproduce Monod's law, as seen in the inset of Figure 8.1.
2. The nutrient composition of the growth media is the main driver of increasing growth rates. Simulate the model to steady state for different values of nutrient qualities. What model species are most impacted by an increase in nutrient quality?
3. As seen in Figure 8.1, the addition of a drug that inhibits protein synthesis results in an upregulation of the ribosomal fraction ϕ_R. Reproduce Figure 8.1. How do the observed results relate to your answer in question 2?

Bibliography

[1] François Jacob and Jacques Monod. Genetic regulatory mechanisms in the synthesis of proteins. *Journal of Molecular Biology*, 3(3):318–356, 1961.

[2] Boris Magasanik. Catabolite repression. In *Cold Spring Harbor Symposia on Quantitative Biology*, volume 26, pages 249–256. Cold Spring Harbor Laboratory Press, 1961.

[3] Aaron Novick and Leo Szilard. Description of the chemostat. *Science*, 112(2920):715–716, 1950.

[4] Suckjoon Jun, Fangwei Si, Rami Pugatch, and Matthew Scott. Fundamental principles in bacterial physiologyhistory, recent progress, and the future with focus on cell size control: a review. *Reports on Progress in Physics*, 81(5):056601, 2018.

[5] Matthew Scott and Terence Hwa. Bacterial growth laws and their applications. *Current Opinion in Biotechnology*, 22(4):559–565, 2011.

[6] Jacques Monod. The growth of bacterial cultures. *Annual Review of Microbiology*, 3(1):371–394, 1949.

[7] SJ Pirt. The maintenance energy of bacteria in growing cultures. *Proceedings of the Royal Society of London. Series B. Biological Sciences*, 163(991):224–231, 1965.

[8] P. van Bodegom. Microbial maintenance: a critical review on its quantification. *Microbial Ecology*, 53 (4):513–523, 2007.

[9] Moselio Schaechter, Ole Maaløe, and Niels O Kjeldgaard. Dependency on medium and temperature of cell size and chemical composition during balanced growth of salmonella typhimurium. *Microbiology*, 19(3):592–606, 1958.

[10] Hans Bremer and Patrick P Dennis. Modulation of chemical composition and other parameters of the cell at different exponential growth rates. *EcoSal Plus*, 3(1), 2008.

[11] Matthew Scott, Carl W Gunderson, Eduard M Mateescu, Zhongge Zhang, and Terence Hwa. Interdependence of cell growth and gene expression: origins and consequences. *Science*, 330(6007):1099–1102, 2010.

[12] Anke Kayser, Jan Weber, Volker Hecht, and Ursula Rinas. Metabolic flux analysis of *Escherichia coli* in glucose-limited continuous culture. I. growth-rate-dependent metabolic efficiency at steady state. *Microbiology*, 151(3):693–706, 2005.

[13] Herbert E Kubitschek, William W Baldwin, and Reinhard Graetzer. Buoyant density constancy during the cell cycle of *Escherichia coli*. *Journal of Bacteriology*, 155(3):1027–1032, 1983.

[14] Herbert E Kubitschek, William W Baldwin, Sally J Schroeter, and Rheinhard Graetzer. Independence of buoyant cell density and growth rate in *Escherichia coli*. *Journal of Bacteriology*, 158(1):296–299, 1984.

[15] Enno R Oldewurtel, Yuki Kitahara, and Sven van Teeffelen. Robust surface-to-mass coupling and turgor-dependent cell width determine bacterial dry-mass density. *Proceedings of the National Academy of Sciences of the USA*, 118(32):e2021416118, 2021.

[16] Frederick C. Neidhardt and H. Edwin Umbarger. *Escherichia coli and Salmonella: Cellular and Molecular Biology. 2nd edition.* American Society of Microbiology (ASM) Press, 1996.

[17] Reinhart Heinrich and Stefan Schuster. *The Regulation of Cellular Systems*. Springer Science & Business Media, 2012.

[18] AH Stouthamer and Corry W Bettenhaussen. Determination of the efficiency of oxidative phosphorylation in continuous cultures of *Aerobacter aerogenes*. *Archives of microbiology*, 102:187–192, 1975.

[19] Bo Xu, Mehmedalija Jahic, and Sven-Olof Enfors. Modeling of overflow metabolism in batch and fed-batch cultures of *Escherichia coli*. *Biotechnology Progress*, 15(1):81–90, 1999.

[20] David L Nelson, Albert L Lehninger, and Michael M Cox. *Lehninger Principles of Biochemistry*. Macmillan, 2008.

[21] Markus Basan, Sheng Hui, Hiroyuki Okano, Zhongge Zhang, Yang Shen, James R Williamson, and Terence Hwa. Overflow metabolism in *Escherichia coli* results from efficient proteome allocation. *Nature*, 528(7580):99–104, 2015.

[22] Goutham N Vemuri, Elliot Altman, DP Sangurdekar, Arkady B Khodursky, and MA Eiteman. Overflow metabolism in *Escherichia coli* during steady-state growth: transcriptional regulation and effect of the redox ratio. *Applied and Environmental Microbiology*, 72(5):3653–3661, 2006.

[23] Ibrahim E Elsemman, Angelica Rodriguez Prado, Pranas Grigaitis, Manuel Garcia Albornoz, Victoria Harman, Stephen W Holman, Johan van Heerden, Frank J Bruggeman, Mark MM Bisschops, Nikolaus Sonnenschein, et al. Whole-cell modeling in yeast predicts compartment-specific proteome constraints that drive metabolic strategies. *Nature Communications*, 13(1):801, 2022.

[24] Sheng Hui, Josh M Silverman, Stephen S Chen, David W Erickson, Markus Basan, Jilong Wang, Terence Hwa, and James R Williamson. Quantitative proteomic analysis reveals a simple strategy of global resource allocation in bacteria. *Molecular Systems Biology*, 11(2):784, 2015.

[25] Conghui You, Hiroyuki Okano, Sheng Hui, Zhongge Zhang, Minsu Kim, Carl W Gunderson, Yi-Ping Wang, Peter Lenz, Dalai Yan, and Terence Hwa. Coordination of bacterial proteome with metabolism by cyclic AMP signalling. *Nature*, 500(7462):301–306, 2013.

[26] Amit Varma and Bernhard O Palsson. Metabolic flux balancing: basic concepts, scientific and practical use. *Bio/Technology*, 12(10):994–998, 1994.

[27] Frederick Carl Neidhardt, John L Ingraham, and Moselio Schaechter. *Physiology of the Bacterial Cell: A Molecular Approach*. Sinauer, Sunderland, MA, 1990.

[28] Ohad Golan. *Metabolic Insights from Coarse-Grained Modeling of Multiple Nutrient Sources*. PhD thesis, ETH Zurich, 2023.

[29] Andrea Y Weiße, Diego A Oyarzún, Vincent Danos, and Peter S Swain. Mechanistic links between cellular trade-offs, gene expression, and growth. *Proceedings of the National Academy of Sciences of the USA*, 112(9):E1038–E1047, 2015.

[30] C.N. Hinshelwood. On the chemical kinetics of autosynthetic systems. *Journal of the Chemical Society*, pages 745–755, 1952.

[31] M. Kafri, E. Metzl-Raz, F. Jonas, and N. Barkai N. Rethinking cell growth models. *FEMS Yeast Research*, 16(7):fow081, 2016.

[32] H. de Jong, S. Casagranda, N. Giordano, E. Cinquemani, D. Ropers, J. Geiselmann, and J.-L. Gouzé. Mathematical modelling of microbes: metabolism, gene expression and growth. *Journal of the Royal Society Interface*, 14(136):2017050, 2017.

[33] F.J. Bruggeman, R. Planqué, D. Molenaar, and B. Teusink. Searching for principles of microbial physiology. *FEMS Microbiology Reviews*, 44(6):821–844, 2020.

[34] D. Molenaar, R. van Berlo, D. de Ridder, and B. Teusink. Shifts in growth strategies reflect tradeoffs in cellular economics. *Molecular Systems Biology*, 5:323, 2009.

[35] T. Zavřel, M. Faizi, C. Loureiro, G. Poschmann, K. Stühler, M. Sinetova, A. Zorina, R. Steuer, and J. Červenó. Quantitative insights into the cyanobacterial cell economy. *eLife*, 8:e42508, 2019.

[36] Benjamin D Towbin, Yael Korem, Anat Bren, Shany Doron, Rotem Sorek, and Uri Alon. Optimality and sub-optimality in a bacterial growth law. *Nature Communications*, 8(1):14123, 2017.